



1               **Impacts of future land use and land cover change on mid-21<sup>st</sup>-**  
2               **century surface ozone air quality: Distinguishing between the**  
3               **biogeophysical and biogeochemical effects**

4  
5  
6   Lang Wang<sup>1,2</sup>, Amos P. K. Tai<sup>1,3,4</sup>, Chi-Yung Tam<sup>1,3</sup>, Mehliyar Sadiq<sup>1,3</sup>, Peng Wang<sup>3</sup>,  
7   Kevin K. W. Cheung<sup>5</sup>

8           1 Institute of Environment, Energy and Sustainability, The Chinese University of  
9   Hong Kong, Hong Kong, China

10          2 Department of Geography and Resource Management, The Chinese University of  
11   Hong Kong, Hong Kong, China

12          3 Earth System Science Programme, Faculty of Science, The Chinese University of  
13   Hong Kong, Hong Kong, China

14          4 Partner State Key Laboratory of Agrobiotechnology, The Chinese University of  
15   Hong Kong, Hong Kong, China

16          5 Department of Environmental Sciences, Macquarie University, Sydney, Australia

17  
18  
19  
20  
21  
22  
23  
24



25

### Abstract

26           Surface ozone (O<sub>3</sub>) is an important air pollutant and greenhouse gas. Land use  
27 and land cover (LULC) is one of the critical factors influencing ozone, in addition to  
28 anthropogenic emissions and climate. LULC change can on the one hand affect ozone  
29 “biogeochemically”, i.e., via dry deposition and biogenic emissions of volatile  
30 organic compounds (VOCs). LULC change can on the other hand alter regional- to  
31 large-scale climate through modifying albedo and evapotranspiration, which can lead  
32 to changes in surface temperature, hydrometeorology and atmospheric circulation that  
33 can ultimately impact ozone “biogeophysically” over local and remote areas. Such  
34 biogeophysical effects of LULC on ozone are largely understudied. This study  
35 investigates the individual and combined biogeophysical and biogeochemical effects  
36 of LULC on ozone, and explicitly examines the critical pathway for how LULC  
37 change impacts ozone pollution. A global coupled atmosphere-chemistry-land model  
38 is driven by projected LULC changes from the present day (2000) to future (2050)  
39 under RCP4.5 and RCP8.5 scenarios, focusing on the boreal summer. Results reveal  
40 that when considering biogeochemical effects only, surface ozone is predicted to have  
41 slight changes by up to 2 ppbv maximum in some areas due to LULC changes. It is  
42 primarily driven by changes in isoprene emission and dry deposition counteracting  
43 each other in shaping ozone. In contrast, when considering the integrated effect of  
44 LULC, ozone is more substantially altered by up to 6 ppbv over several regions,  
45 reflecting the importance of biogeophysical effects on ozone changes. Furthermore,  
46 large areas of these ozone changes are found over the regions without LULC changes  
47 where the biogeophysical effect is the only pathway for such changes. The  
48 mechanism is likely that LULC change induces a regional circulation response, in  
49 particular the formation of anomalous stationary high-pressure systems, shifting of



50 moisture transport, and near-surface warming over the middle-to-high northern  
51 latitudes in boreal summer, owing to associated changes in albedo and surface energy  
52 budget. Such temperature changes then alter ozone substantially. We conclude that  
53 the biogeophysical effect of LULC is an important pathway for the influence of  
54 LULC change on ozone air quality over both local and remote regions, even in  
55 locations without significant LULC changes. Overlooking the impact of  
56 biogeophysical effect may cause evident underestimation of the impacts of LULC  
57 change on ozone pollution.

58

59 **Keywords:** ozone pollution; land use and land cover change; biogeochemical effects;  
60 biogeophysical effects

61



## 62 1. Introduction

63 Surface ozone (O<sub>3</sub>), as a harmful air pollutant, has negative consequences for  
64 human health (WHO, 2005; Jerrett et al., 2009; Malley et al., 2017), decreases plant  
65 gross primary productivity (e.g., Yue and Unger 2014), and leads to substantial  
66 reductions in global crop yields (Avnery et al., 2011; Tai et al., 2014; Tian et al.,  
67 2016; Tai and Val Martin, 2017; Mills et al., 2018). It is also an important greenhouse  
68 gas, contributing to climate change (Myhre et al., 2013). Surface ozone is produced  
69 by the photooxidation of precursors including carbon monoxide (CO), methane  
70 (CH<sub>4</sub>), and other non-methane volatile organic compounds (NMVOCs) in the  
71 presence of nitrogen oxides (NO<sub>x</sub>). These precursors are both generated by human  
72 activities and naturally emitted from vegetation and soils. Surface ozone is lost mostly  
73 by photolysis and via dry deposition onto vegetation mainly in the form of leaf  
74 stomatal uptake. Depending on all of these production and loss mechanisms, its  
75 concentration is highly sensitive to changes in natural and anthropogenic emissions of  
76 precursors (Wang et al., 2011), land use and land cover (LULC) (Ganzeveld et al.,  
77 2010; Val Martin et al., 2015; Fu and Tai, 2015) and climate (Jacob and Winner,  
78 2009; Fiore et al., 2012; Schnell et al., 2016). Recent studies found that decreases in  
79 anthropogenic emissions alone might not necessarily decrease ozone in some polluted  
80 regions if factors such as climatic and LULC changes act to enhance ozone and offset  
81 emission control efforts (Zhou et al., 2013; Zhang et al., 2014; Xue et al., 2014).

82 Changes in LULC can modify ozone concentration by altering key drivers of  
83 ozone such as biogenic VOC emissions and dry deposition (e.g., Wong et al., 2018).  
84 These can be referred to as “biogeochemical effects” of LULC on ozone (as opposed  
85 to “biogeophysical effects”, which will be discussed next), because these processes  
86 entail directly modifying the biosphere-atmosphere exchange of gases and particles



87 that alters atmospheric composition including ozone itself. Here we limit the  
88 “biogeochemical effects” of LULC on ozone to processes that influence ozone  
89 directly in a given climate, including biogenic VOC emission and the dry deposition  
90 of ozone and its precursors; climatic changes that can arise from LULC disturbances  
91 of the biogeochemical cycles are not the focus.

92 LULC changes can modify the spatial pattern and magnitude of isoprene  
93 emission due to their strong dependence on vegetation type and leaf density  
94 (Guenther et al., 2012). For instance, Lathière et al. (2006) found as much as a 29%  
95 decrease in global isoprene emission from a scenario in which 50% tropical trees are  
96 replaced by grasses. Heald and Spracklen (2015) estimated the net effect of LULC  
97 changes under future anthropogenic influences as a decrease of 12–15% in global  
98 isoprene emission. These changes in isoprene emission can in turn modify ozone  
99 concentration. For example, Tai et al. (2013) found that LULC projections in the  
100 Intergovernmental Panel on Climate Change (IPCC) A1B scenario with widespread  
101 crop expansion could reduce isoprene emission by ~10% globally compared with  
102 LULC at present. Such a reduction could correspondingly lead to an up to 4 ppbv of  
103 ozone decrease in the eastern US and western Europe, and an up to 6 ppbv increase in  
104 South and Southeast Asia, whereby the difference in the sign of responses is driven  
105 primarily by the different ozone production regimes.

106 Dry deposition is another key factor modulating ozone. Dry deposition is the  
107 most efficient over densely vegetated regions via the stomatal uptake of ozone and its  
108 precursors, and LULC changes can alter these fluxes. Kroeger et al. (2013) found that  
109 reforestation over peri-urban areas in Texas, USA, could effectively enhance dry  
110 deposition, resulting in decreases in ozone and its precursors. Fu and Tai (2015) found  
111 that LULC change driven by climate and CO<sub>2</sub> changes could overall enhance dry

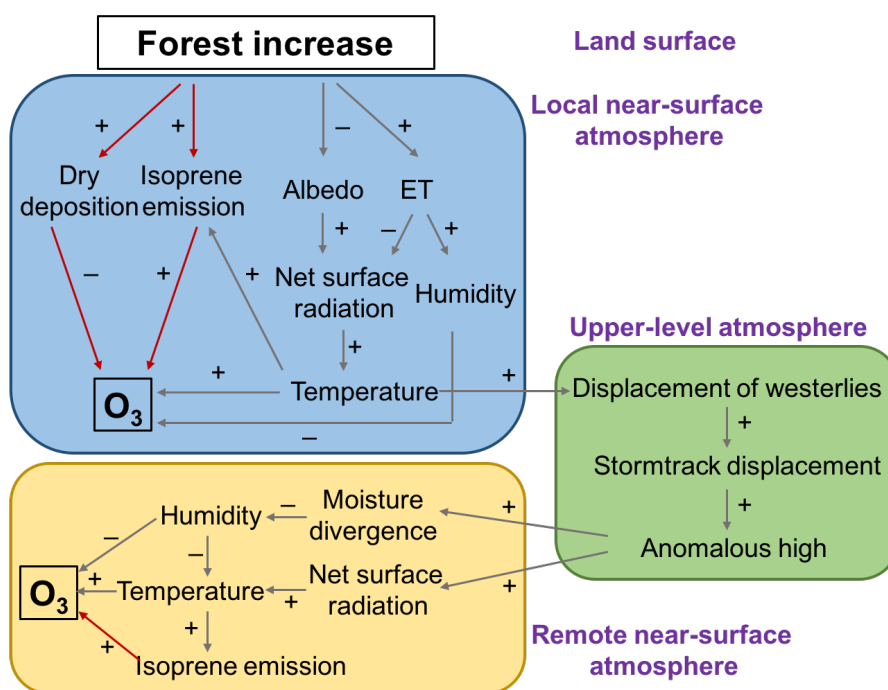


112 deposition and decrease ozone by up to 4 ppbv in East Asia during the past three  
113 decades. The dry deposition enhancement mostly arises from climate- and CO<sub>2</sub>-  
114 induced increase in leaf area index (LAI), which more than offsets the compensating  
115 effect of cropland expansion. The relative importance of isoprene emission and dry  
116 deposition, which could have counteracting effects on ozone given the same LULC  
117 change, is strongly dependent on local NO<sub>x</sub> concentrations and vegetation type (Wong  
118 et al., 2018).

119 Changes in LULC can also affect weather and climate over local and remote  
120 regions by perturbing the biosphere-atmosphere exchange of water and energy fluxes  
121 (e.g. Betts, 2001; Bonan, 2016; Pitman et al., 2009). Furthermore, studies have  
122 identified significant contributions of LULC changes to changes in larger-scale  
123 circulation pattern, sea-level pressure and geopotential height up to the upper  
124 troposphere (Henderson-Sellers et al. 1993; Chase et al., 1996; Swann et al., 2012).  
125 Such a modification of the overlying meteorological environment and climate induced  
126 by LULC changes and the associated exchange of momentum, heat and moisture  
127 between the land and atmosphere can be defined as “biogeophysical effects” of  
128 LULC. Such effects can further alter surface ozone on local to pan-regional scales  
129 (Jiang et al., 2008; Ganzeveld et al., 2010; Wu et al., 2012), and we shall call these  
130 and related pathways the biogeophysical effects of LULC on ozone. In particular, a  
131 LULC-induced increase in surface temperature could (1) accelerate peroxyacetyl  
132 nitrate (PAN) decomposition into NO<sub>x</sub> (Jacob and Winner, 2009; Doherty et al., 2013;  
133 Pusede et al., 2015), (2) increase biogenic VOCs emissions from vegetation  
134 (Guenther et al., 2012; Wang et al., 2013; Squire et al., 2014), and (3) lead to more  
135 water vapor in air that tends to increase ozone destruction (Jacob and Winner, 2009)  
136 (Fig. 1). The net effect of higher temperatures is almost always ubiquitously an



137 enhancement of ozone levels reported from both observational (e.g., Porter et al.,  
138 2015; Pusede et al., 2015) and modeling (e.g., Shen et al., 2016; Lin et al., 2017)  
139 studies in many polluted regions.  
140



141  
142 Figure 1. Schematic diagram showing the biogeochemical and biogeophysical effects of land use and  
143 land cover (LULC) change on surface ozone, using a case where forest coverage increases (e.g., under  
144 the RCP4.5 scenario) as an example. Red arrows indicate biogeochemical effects and grey arrows  
145 indicate biogeophysical effects. We focus on processes initiated at the land surface by LULC changes,  
146 and the corresponding responses in local near-surface atmosphere (blue box), upper-level atmosphere  
147 (green box) and remote near-surface atmosphere (yellow box).

148  
149 The LULC biogeophysical effects have thus far been largely unexplored,  
150 though biogeochemical effects of LULC have been examined by a number of studies  
151 (Wu et al., 2012; Fu and Tai, 2015; Heald and Geddes, 2016). Only a few recent



152 studies have implicitly included such biogeophysical effects of LULC in their coupled  
153 land-atmosphere models when assessing the impacts of LULC changes on surface  
154 ozone. Val Martin et al (2015) studied the integrated effects of LULC change on  
155 surface ozone using future LULC change scenarios, and found an increase of 2–3  
156 ppbv from 2000 to 2050 over US national parks. Ganzeveld et al. (2010) also  
157 calculated the future LULC changes from 2000 to 2050, and found that an increase in  
158 boundary-layer ozone mixing ratios by up to 20% over the tropics. However, these  
159 studies did not distinguish between the roles of biogeophysical vs. biogeochemical  
160 effects, or decipher the physics and relative importance of various mechanisms behind  
161 the integrated effects.

162         The aim of this study is to investigate how and to what extent global LULC  
163 changes could affect surface ozone in the near future by investigating and  
164 distinguishing between the biogeochemical, biogeophysical and integrated effects of  
165 LULC changes. We suggest a new line of biogeophysical pathways linking LULC  
166 changes to surface ozone, and also consider biogeochemical pathways through  
167 isoprene emission and dry deposition changes caused by LULC changes. In particular,  
168 over the regions without significant LULC changes but showing substantial ozone  
169 changes, we find that the biogeophysical effects arising from LULC-induced  
170 atmospheric circulation changes can be dominant and could be isolated from the  
171 integrated effects. LULC change is one of the key strategies for climate change  
172 mitigation, but meanwhile has substantial impacts on ozone pollution. Understanding  
173 its comprehensive pathways on surface ozone can help provide important references  
174 for integrated air quality and LULC management in the future.

175





176 **2. Data and methods**

177 *2.1 Modeling framework*

178 To simulate the impacts of LULC change on surface ozone, we use the  
179 Community Earth System Model (CESM) version 1.2  
180 (<http://www.cesm.ucar.edu/models/>), which is a comprehensive global model that  
181 couples different independent components for the atmosphere, land, ocean, sea ice,  
182 land ice and river runoff (Lamarque et al., 2012). The atmospheric component is the  
183 Community Atmosphere Model version 4 (CAM4), which uses a finite-volume  
184 dynamical core with comprehensive tropospheric and stratospheric chemistry (CAM-  
185 Chem). Chemical mechanisms are based on the Model for Ozone and Related  
186 chemical Tracers (MOZART) version 4 (Emmons et al., 2010). For the land  
187 component, the Community Land Model (CLM) version 4.5 (Oleson, 2013) considers  
188 16 Plant Function types (PFTs) (Lawrence et al., 2011), and prescribes the total leaf  
189 area index (LAI), the PFT distribution and PFT-specific seasonal LAI derived from  
190 Moderate Resolution Imaging Spectroradiometer (MODIS) observations. We use the  
191 Satellite Phenology (SP) mode of CLM4.5, which prescribes vegetation structural  
192 variables including LAI and canopy height; active biogeochemical cycling in  
193 terrestrial ecosystems is not turned on.

194 In CLM4.5, biogenic VOC emissions are computed using the Model of  
195 Emissions of Gases and Aerosols from Nature (MEGAN) version 2.1 (Guenther et al.,  
196 2012), accounting for the major known processes controlling biogenic VOC  
197 emissions from terrestrial ecosystems, such as effects of temperature, solar radiation,  
198 soil moisture, leaf age, CO<sub>2</sub> concentrations, and vegetation species and density.  
199 Biogenic VOC emissions in MEGAN are allowed to respond interactively to changes  
200 of these processes. Dry deposition of gases and aerosols are computed based on the



201 multiple resistance approach of Wesely (1989), updated by Emmons et al. (2010),  
202 Lamarque et al. (2012) and Val Martin et al. (2014). In the scheme, dry deposition  
203 velocity is the inverse of aerodynamic resistance ( $R_a$ ), sublayer resistance ( $R_b$ ) and  
204 bulk surface resistance ( $R_c$ ), whereby  $R_c$  includes a combination of resistances from  
205 vegetation (including stomatal resistance), lower canopy, and ground with specific  
206 values for different land types. Correspondingly, dry deposition velocity in the  
207 scheme responds to primarily meteorological and ecophysiological conditions; in  
208 particular, Val Martin et al. (2014) updated stomatal resistance in the default dry  
209 deposition calculation such that now it is directly coupled to photosynthetic  
210 calculation in CLM. Soil  $\text{NO}_x$  emissions are dependent on soil moisture, soil  
211 temperature and vegetation cover (Emmons et al., 2010 ; Yienger and Levy, 1995),  
212 while biomass burning emissions and anthropogenic emissions of ozone precursors,  
213 are prescribed by inventory at present-day levels.

214 The coupled CAM-Chem-CLM model configuration of CESM can be run  
215 with prescribed meteorology to drive atmospheric chemistry-only simulations  
216 (hereafter as dynamical Off-line mode), or with interactive, dynamically simulated  
217 meteorology using CAM4 (hereafter as On-line mode). Here we use the Goddard  
218 Earth Observing System Model Version 5 (GEOS-5)  
219 (<https://rda.ucar.edu/datasets/ds313.0/>) (Tilmes, 2016) assimilated meteorology to  
220 drive the Off-line mode, which has 56 vertical levels to match the resolution. On the  
221 other hand, CAM4 has 26 vertical levels. Both of them vertically span between the  
222 Earth's surface and the 4 hPa level, with horizontal resolution of  $1.9^\circ \times 2.5^\circ$  is used.  
223 For the coupled configuration with dynamic meteorology, concentrations of long-  
224 lived greenhouse gases including  $\text{CO}_2$ ,  $\text{CH}_4$ , and  $\text{N}_2\text{O}$  are prescribed at present-day  
225 levels for all simulations. Climatic changes that may arise from LULC disturbances of



226 the terrestrial carbon and nitrogen cycles are not the focus of this study, which aims to  
227 delineate the more immediate responses of surface ozone to LULC change.

228 The CAM-Chem-simulated atmospheric chemistry has been extensively  
229 evaluated and documented (e.g., Lamarque et al., 2012). In general, CAM-Chem can  
230 reasonably replicate observed values at individual sites (CASTNET for US and  
231 EMEP for Europe) (Lamarque et al., 2012; Val Martin et al., 2014; Sadiq et al.,  
232 2017), mid- and upper-tropospheric observations (Lamarque et al., 2010) albeit with a  
233 general overestimation; and the performance is comparable to other global and  
234 regional models (Lapina et al., 2014; Parrish et al., 2014). Uncertain emissions, coarse  
235 resolution (Lamarque et al., 2012), misrepresentation of dry deposition process and  
236 overestimation of stomatal resistance are all likely factors contributing to these high  
237 biases.

### 238 *2.2 Present and future LULC scenarios*

239 For the present-day LULC distribution, satellite phenology based on MODIS  
240 and a cropping dataset from Ramankutty et al. (2008) are used (see Lawrence et al.,  
241 2011). The cropping dataset combines agricultural inventory data and two satellite-  
242 derived land products. For the future LULC, projections based on the Representative  
243 Concentration Pathways (RCP) 4.5 and 8.5 scenarios are adopted (van Vuuren et al.,  
244 2011). Both are computed using Integrated Assessment Models (IAM) for the Phase 5  
245 of the Coupled Model Intercomparison Project (CMIP5) community, incorporating  
246 anthropogenic transformation and activities associated with carbon releases (e.g.,  
247 wood harvest). These LULC projections are internally consistent with the  
248 corresponding emission scenarios and development pathways for the Fifth  
249 Assessment Report (AR5) of Intergovernmental Panel on Climate Change (IPCC)  
250 (Taylor et al., 2012). In general, the RCP4.5 LULC change has the most extensive use



251 of land management as a carbon mitigation strategy, with the expansion of forest  
252 areas combined with large reductions in croplands and grasslands. The RCP8.5 LULC  
253 change has the least effective use of land management for carbon mitigation, with  
254 large expansion in both croplands and grasslands together with substantial forest  
255 losses.

256 Both present-day and future LULC are transformed into PFTs changes for  
257 implementation into CESM (Lawrence et al., 2012; Oleson et al., 2013). The long-  
258 term time series of LULC changes span through the historical (1850–2005) and future  
259 (2006–2100) periods in 5-year intervals (Riahi et al., 2007; van Vuuren et al., 2007;  
260 Wise et al., 2009a), and are then interpolated and harmonized with smooth transitions  
261 on the annual timescale (Hurtt et al., 2011). For this work, we focus on LULC  
262 changes from the present-day (2000) to future (2050) period.

### 263 *2.3 Model experiments*

264 We have two sets of configuration, Off-line mode and On-line mode, with  
265 eight simulations to investigate the impacts of LULC changes on surface ozone (see  
266 Table 1). We focus on boreal summer month (June-July-August, JJA) averages as this  
267 is the period when ozone pollution is generally the most severe in the Northern  
268 Hemisphere. The first set of simulations in Off-line mode is used to quantify the  
269 effects of future projected LULC changes alone on surface ozone with prescribed  
270 meteorology of the present day. Surface ozone would respond to LULC change only  
271 through biogeochemical effects that mainly include changes in dry deposition velocity  
272 and isoprene emissions due to different LULC change scenarios without  
273 meteorological responses to LULC changes. The Off-line mode includes control run  
274 (Off-line\_CTL) using present-day (year 2000) LULC distribution, and two future  
275 simulations Off-line\_45 and Off-line\_85, with year-2050 LULC distribution



276 following RCP4.5 and RCP8.5, respectively. All three experiments are time-sliced  
277 simulations using prescribed GEOS-5 meteorology from 2004 to 2017 for 14 years  
278 allowing for interannual climate variability, and we use the last 10-year averages for  
279 analysis.  
280



281

Case Name	Land forcing	Meteorology	Simulated years	Other forcing
1 Off-line_CTL	Present-day (2000) land use and land cover (LULC) map	GEOS-5 reanalysis (2004-2017)	14 years The last 10 years average for analysis	- Present-day (2000) well-mixed greenhouse gases and short-lived gases and aerosols, anthropogenic emissions;
2 Off-line_45	2050 RCP4.5 scenario future LULC map in time slice	GEOS-5 reanalysis (2004-2017)	14 years The last 10 years average for analysis	- Present-day (2000) monthly mean sea surface temperature and sea ice
3 Off-line_85	2050 RCP8.5 scenario future LULC map in time slice	GEOS-5 reanalysis (2004-2017)	14 years The last 10 years average for analysis	
4 On-line_CTL	Present-day (2000) LULC map	Simulated online	55 years The last 10 years average for analysis	
5 On-line_45	2000-2005 historical, 2006-2054 RCP4.5 scenario transient LULC map	Simulated online	55 years The last 10 years average for analysis	
6 On-line_85	2000-2005 historical, 2006-2054 RCP8.5 scenario transient LULC map	Simulated online	55 years The last 10 years average for analysis	
7 On-line_45TS	2050 RCP4.5 scenario future LULC map in time slice	Simulated online	55 years The last 10 years average for analysis	
8 On-line_85TS	2050 RCP8.5 scenario future LULC map in time slice	Simulated online	55 years The last 10 years	

282

283

Table 1. List of model experiments. There is one ensemble member considered for each “On-line” model

284

simulation; for Cases 4, 7 and 8, since the same annual forcings are used for 55 years of simulation, each year of

285

simulation can be treated as one of the 55 pseudo-ensemble members.



286           The second set of five On-line mode simulations is performed in order to  
287 assess the integrated and biogeophysical effects on surface ozone caused by future  
288 projected LULC changes, considering also the effects of the resulting meteorological  
289 changes. The first experiment On-line\_CTL, reflects present-day conditions and uses  
290 LULC forcing for year 2000. The second and third experiments, referred to as On-  
291 line\_45 and On-line\_85, are transient simulations performed continuously from year  
292 2000 to 2054 using transient LULC maps projected for the RCP4.5 and RCP8.5  
293 scenarios, respectively. The fourth and fifth experiments, On-line\_45TS and On-  
294 line\_85TS, are time-sliced simulations using 2050 LULC distribution following  
295 RCP4.5 and RCP8.5, respectively. These two experiments are designed for paralleled  
296 comparison with Off-line mode simulations, and for additional comparison between  
297 the impacts of LULC using time-sliced runs and transient runs on ozone pollution and  
298 related pathways in the model. All five On-line experiments are run for 55 years, and  
299 the last ten years are used for analysis after modeled variables have attained a quasi-  
300 steady state. Our experiments all start from an equilibrium (spun-up) state for the year  
301 2000; the spun-up state uses offline CLM run for 50 years forced by the cycling year  
302 2000 of the Qian et al. (2006) atmospheric conditions. All simulations are performed  
303 with prescribed sea surface temperature and sea-ice cover following the HadISST data  
304 set (Rayner et al., 2003) at the year-2000 level. Long-lived greenhouse gases and thus  
305 the radiative forcing from them are kept at present-day conditions (year 2000) to  
306 isolate the effects of LULC changes only.

307           These eight sets of model configuration allow us to separate and examine: (1)  
308 biogeochemical effects of LULC changes on surface ozone, (2) biogeophysical effects  
309 on surface ozone, and (3) the integrated effects induced by LULC change on surface  
310 ozone and its precursors and dry deposition.

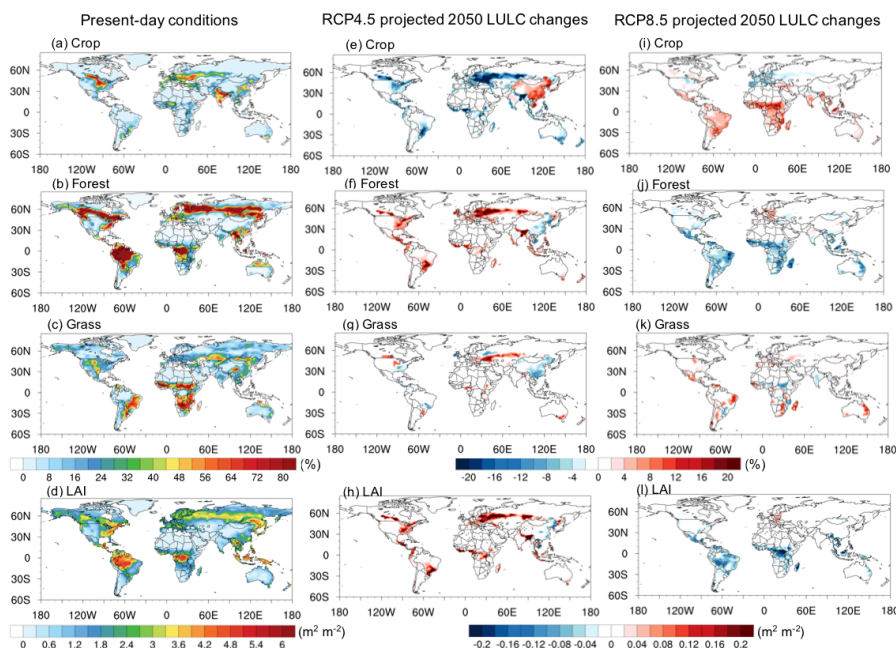


311 **3. Results**

312 *3.1 Projected LULC changes from 2000 to 2050*

313 Fig. 2 shows the global distribution of present-day (year 2000) PFTs and  
314 future projected changes (2000 to 2050) following RCP4.5 and RCP8.5 for three  
315 major LULC categories. The future LULC changes in RCP4.5 are characterized by  
316 extensive forest expansion (Figs. 2e, f, g). Transition from present-day to 2050 in  
317 RCP4.5 highlights the global growth of forest from 71.8 million to 74.0 million km<sup>2</sup>,  
318 at the expense of croplands (from 14.7 million to 12.3 million km<sup>2</sup>); grasslands  
319 slightly increase in area from 33.7 million to 33.8 million km<sup>2</sup>. The net increase of 2.2  
320 million km<sup>2</sup> of forests is consistent with that provided by Hurtt et al. (2011),  
321 Lawrence et al. (2012) and Heald and Geddes (2016). Fig. 2e also illustrates cropland  
322 area increases over Southeast Asia, India and China. Such increases are due to more  
323 bioenergy crop production for the purpose of climate change mitigation, economic  
324 advantages from agriculture productivity growth, lower regional land prices, and  
325 availability of undeveloped lands in these developing regions (Wise et al., 2009b;  
326 Thomson et al., 2011). In contrast, regions such as Europe, US and Canada, undergo  
327 extensive reforestation. RCP8.5 LULC changes are characterized by extensive  
328 cropland expansion (Figs. 2i, j, k), driven mainly by a large increase in the global  
329 population and a slow increase in crop yields due to a slow rate of exchange of  
330 technology globally (Riahi et al., 2011). Cropland expansion occurs largely over the  
331 tropical belt (30°N-30°S) at the expense of forest reduction. The total increases in  
332 croplands are by 1.8 million km<sup>2</sup>, and forest area decreases by 2.5 million km<sup>2</sup>.  
333





334

335 Figure 2. Present-day (2000) land use and land cover (LULC) by percentage of land coverage and total  
336 leaf area index (LAI) (left), and their changes from 2000 to 2050 under RCP4.5 (middle) and RCP8.5  
337 (right) scenarios for the boreal summer (June-July-August) (units at the right side of the color bar).

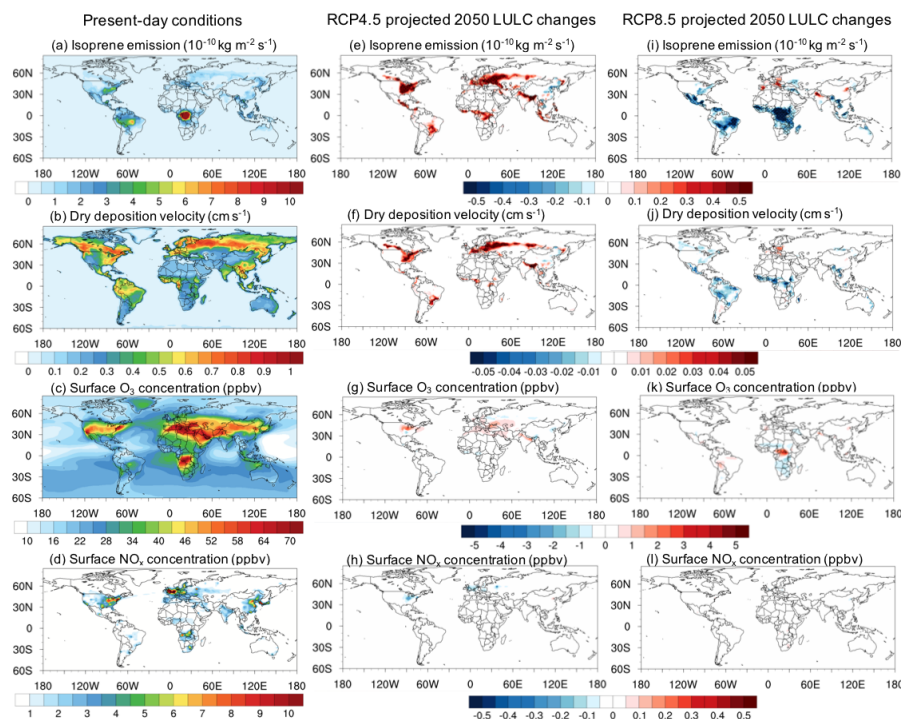
338 Plant function types in CESM are here grouped into three major categories: crop, forest and grass.

339 The present-day LAI and its changes associated with the future projected  
340 LULC changes are shown in Figs. 2d, 2h and 2i. Forest expansion leads to increases  
341 in LAI, vice versa. For RCP4.5, due to the widespread reforestation and afforestation  
342 except in East Asia, LAI increases significantly. Particularly over Europe and the US,  
343 the absolute increase in LAI is  $> 0.1$ . For RCP8.5, LAI generally declines with intense  
344 reductions over the tropical regions.

### 345 3.2 Biogeochemical effects of LULC changes on surface ozone

346

347



348

349 Figure 3. Simulated present-day (2000) isoprene emission, dry deposition and surface ozone  
350 concentration (left) and their changes from 2000 to 2050 under RCP4.5 (middle) and RCP8.5 projected  
351 LULC changes for the boreal summer (June-July-August). These are results from Off-line runs with  
352 prescribed meteorology; i.e., meteorological variables do not respond to LULC changes.

353 Using the Off-line configuration we find that isoprene emission changes  
354 correspond closely with the LULC changes in each future scenario from 2000 to 2050  
355 (Figs. 3e, i). For RCP4.5, isoprene emission increases over the regions with forest  
356 expansion, including the US, Europe and some tropical regions, but decreases over  
357 East Asia. Such isoprene emission increases are primarily driven by forest expansion,  
358 since forest PFTs typically emit much more isoprene than crops and grasses  
359 (Guenther et al., 2012). For RCP8.5, isoprene emission decreases over the tropics  
360 with slight increases over Europe, north China and north India, largely due to forest  
361 reduction in this scenario.



362            Table 2 summarizes the absolute percentage and value change of the annual  
363    global isoprene emission. The simulated present-day annual global isoprene is 353.8  
364    Tg C yr<sup>-1</sup>, in the middle of the range 308–678 Tg C yr<sup>-1</sup> summarized by Guenther et  
365    al. (2012).

366            For the RCP4.5 LULC change, the annual global isoprene emission increases  
367    by 5.2%, but it decreases by 11.8% for RCP8.5. The isoprene emission changes are in  
368    line with these studies by Heald et al. (2008) and Wu et al. (2012), who estimated a  
369    decrease of 12–15% in global isoprene emission under the net biogeochemical effect  
370    of future LULC changes (A1B and A2 scenarios).

371



372

		Isoprene emissions (TgC yr <sup>-1</sup> )	% change	Ozone dry depositional sink (Tg yr <sup>-1</sup> )	% change
	Off-line_CTL	353.8		886.8	
Off-line	Off-line_45	372.3	5.2	895.4	1.0
	Off-line_85	311.9	-11.8	879.8	-0.8
	On-line_CTL	419.4		969.7	
On-line	On-line_45	433.6	3.4	973.3	0.4
	On-line_85	386.1	-7.9	964.7	-0.5
	On-line_45TS	434.6	3.6	975.9	0.6
	On-line_85TS	383.8	-8.5	961.7	-0.8

373

374 Table 2. Summertime average (June-July-August) global isoprene emission and ozone dry-depositional sink as  
 375 influenced by future LULC changes in the RCP4.5 and RCP8.5 scenarios; shown separately are changes in  
 376 prescribed meteorology (biogeochemical effects only) and coupled atmosphere-chemistry-land configurations  
 377 (both biogeochemical and biogeophysical effects).



378 Fig. 3f shows that LULC changes in the RCP4.5 scenario have enhanced dry  
379 deposition velocity over most regions where forests have expanded. Forest with both  
380 large LAI and high surface roughness often provides the highest dry deposition  
381 velocity amongst all PFTs (Emmons et al., 2010; Lamarque et al., 2012). The most  
382 dramatic changes occur in Europe where local maximum changes occur in LULC  
383 between forests and croplands. Local decreases over East Asia are the result of  
384 deforestation. For RCP8.5, dry deposition velocity decreases mostly over the regions  
385 where tropical forests are replaced by croplands (Fig. 3j). Equatorial Africa and the  
386 Amazon experience the largest decrease in dry deposition velocity relative to present-  
387 day conditions. Some increases over Western Europe are the result of local  
388 reforestation.

389 The globally averaged change in the dry-depositional sink is around 1%  
390 (Table 2). Local dry deposition velocity changes within  $0.05 \text{ cm s}^{-1}$ . The value of dry  
391 deposition velocity change is in line with previous studies exploring future 2050  
392 LULC changes alone on the dry deposition velocity of ozone (e.g. Verbeke et al.,  
393 2015), though our results show slightly larger changes due to larger LAI differences  
394 between forests and crops/grasses during the boreal summer compared with their  
395 annual mean values of differences from Verbeke et al. (2015).

396 Figs. 3g and 3k show the impacts of future projected LULC changes on  
397 surface ozone. LULC changes under RCP4.5 with massive forest expansion increase  
398 isoprene emission that could increase surface ozone, but also enhance dry deposition  
399 velocity that could reduce surface ozone. The overall changes in surface ozone are  
400 thus generally small due to these compensating effects. There are a few regions with  
401 surface ozone changes by up to 2 ppbv. In particular, over the US, opposite surface  
402 ozone changes are seen in RCP4.5: an increase in the northeast US and a decrease in



403 the southeast US despite of the fact that both changes are driven by forest expansion  
404 (Fig. 3g). Such a contrasting pattern is shaped by the local atmospheric chemical  
405 conditions related to O<sub>3</sub>-NO<sub>x</sub>-VOC chemistry. The northeast US is a high-NO<sub>x</sub> region  
406 (Fig. 3d), and increases in isoprene emission result in enhanced ozone, more than  
407 offsetting the effect of increasing dry deposition velocity. In contrast, the southeast  
408 US is a high-isoprene-emitting region; additional isoprene may react with ozone and  
409 NO<sub>x</sub>, thereby suppressing surface ozone production (Kang et al., 2003; von Kuhlmann  
410 et al., 2004; Fiore et al., 2005; Pfister et al., 2008; see also discussion in Section 4).  
411 Together with the increase in dry deposition velocity, overall there is a decrease of  
412 surface ozone. Similar to the northeastern US conditions, southern Europe,  
413 northeastern India and northern China are also high-NO<sub>x</sub> regions. The area with ozone  
414 changes (Fig. 3g) corresponds well with changes in local isoprene emission (Fig. 3e)  
415 rather than in dry deposition velocity (Fig. 3f).

416 Under the RCP8.5 scenario with substantial cropland and grassland expansion,  
417 decrease in isoprene emission and dry deposition again offset each other in  
418 controlling surface ozone in high-NO<sub>x</sub> regions. Surface ozone concentration decreases  
419 by around 1 ppbv over the north-central and southern Africa, but increases by up to 2  
420 ppbv over equatorial Africa and central South America (Fig. 3k). In particular, the  
421 area with enhanced ozone in these regions corresponds well with reductions in  
422 isoprene emission and dry deposition together. Equatorial Africa is a high-isoprene-  
423 emitting, low-NO<sub>x</sub> region, thus decreases of isoprene emission together with reduced  
424 dry deposition would lead to enhanced ozone.

### 425 *3.3 Biogeophysical effects of LULC change on surface ozone*

426 Next we examine results from the On-line simulations, which allow us to  
427 assess the impacts of LULC changes on surface ozone when the overlying



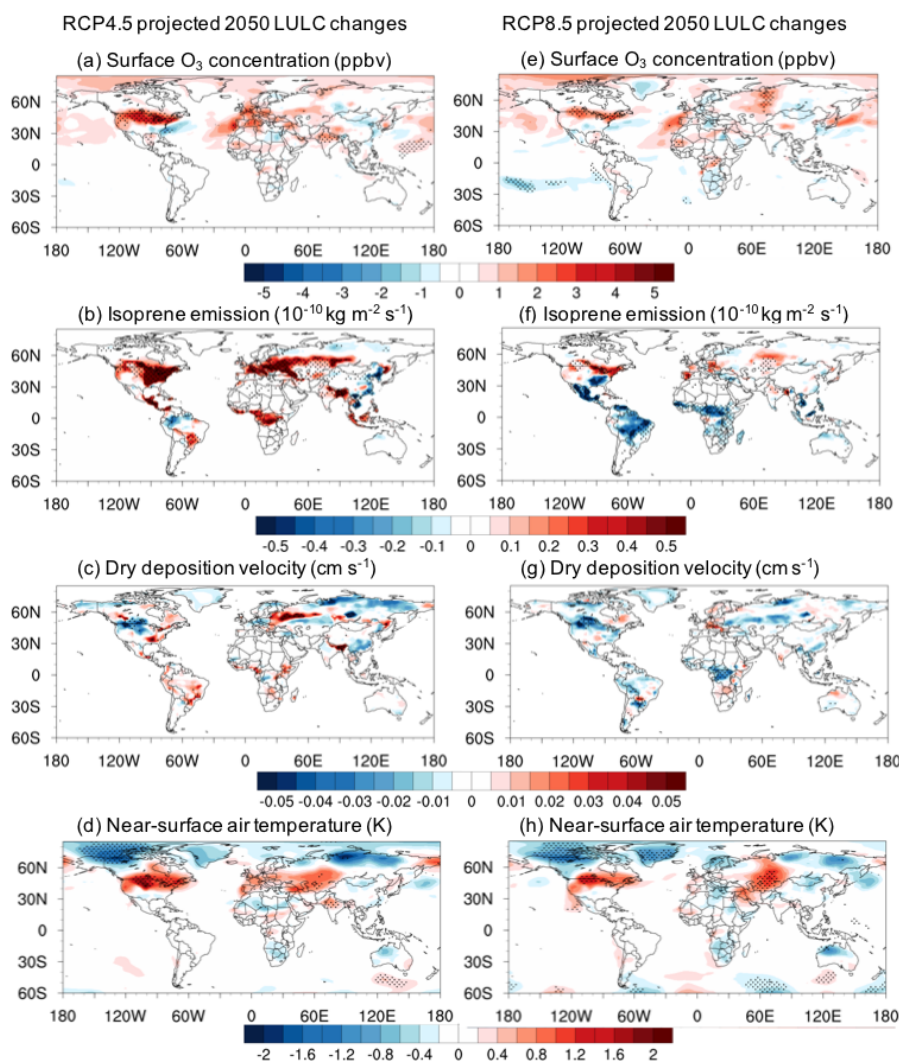
428 meteorological environment is also modified by LULC changes. The simulated  
429 changes in surface ozone is in the range from  $-3$  to  $+6$  ppbv (Figs. 4a, e), which are  
430 substantial and comparable to other studies that also considered meteorological  
431 responses to LULC changes (Ganzeveld et al., 2010; Val Martin et al., 2015), and to  
432 surface ozone responses to changes in anthropogenic emissions and climate (Jacob  
433 and Winner, 2009). This confirms the important roles of LULC in modulating surface  
434 ozone. Furthermore, the magnitude of ozone changes in On-line simulations is overall  
435 larger than those in Off-line simulations, which consider biogeochemical effects only,  
436 indicating the importance of complications from the changing meteorological  
437 environment in response to LULC changes.

438         In contrast to the clear, localized signals in ozone changes in response to  
439 LULC changes through biogeochemical pathways, surface ozone changes are more  
440 complex when biogeophysical pathways are also involved (Figs. 4a, e). Most  
441 importantly, both local and remote ozone changes can be discerned. The patterns of  
442 ozone changes correspond to patterns of isoprene emission (Figs. 4b, f) and dry  
443 deposition (Figs. 4c, g) changes to some extent. On the other hand, they correlate well  
444 with patterns of temperature change, indicating that the biogeophysical drivers that  
445 modify surface temperature may play the most dominant roles. Figs. 4d and 4h show  
446 simulated changes in near-surface air temperature (below the 850 hPa level) from  
447 2000 to 2050. Regional-scale temperature changes of up to 2 K are found. Such  
448 magnitudes of temperature anomalies induced by LULC changes are in line with  
449 those from previous experiments (Lawrence et al., 2012; Brovkin et al., 2013). Both  
450 local and remote temperature changes could be driven by LULC changes. Over the  
451 regions where temperature increases, surface ozone increases correspondingly.



452           Furthermore, changes in isoprene emission also correlate with temperature  
453 changes (Figs. 4b, d; Figs. 4f, h), showing that isoprene emission generally increases  
454 in regions with warmer temperatures. Isoprene emission also increases in regions with  
455 forest expansion reflecting the biogeochemical mentioned in Section 3.2 and the  
456 integrated effects of LULC. Moreover, the changes in dry deposition velocity (Figs.  
457 4c, g) also correlate to meteorological changes (through stomatal responses to  
458 drier/wetter conditions) as well as LULC changes. Table 2 shows the changes in  
459 global annual isoprene emission and dry-depositional sink in two scenarios between  
460 2000 and 2050 when considered LULC changes. In particular, the On-line mode  
461 values of isoprene emission change are smaller than the Off-line values by around 2%  
462 in each scenario, indicating the non-negligible role of biogeophysical effects on  
463 isoprene emission via partly offsetting the biogeochemical effects.





464

465 Figure 4. Simulated 2000-to-2050 changes in surface ozone, isoprene emission, dry deposition velocity  
466 and near-surface air temperature with atmosphere-chemistry-land coupled configurations for the boreal  
467 summer, under two future scenarios (RCP4.5 and RCP8.5). These and all following results are from the  
468 On-line runs with dynamic meteorological responses to LULC changes.

469 Thus, changes in ozone can be caused by both biogeochemical and  
470 biogeophysical effects of LULC; furthermore, both effects are highly coupled with  
471 each other. We find that in particular the biogeophysical effects of LULC changes  
472 play critical roles in modulating surface ozone. Hereafter, we focus on the broad



473 regions of North America, Europe and Asia (India and China), in order to elucidate  
474 the origins of surface ozone changes in response to LULC-induced meteorological  
475 changes.

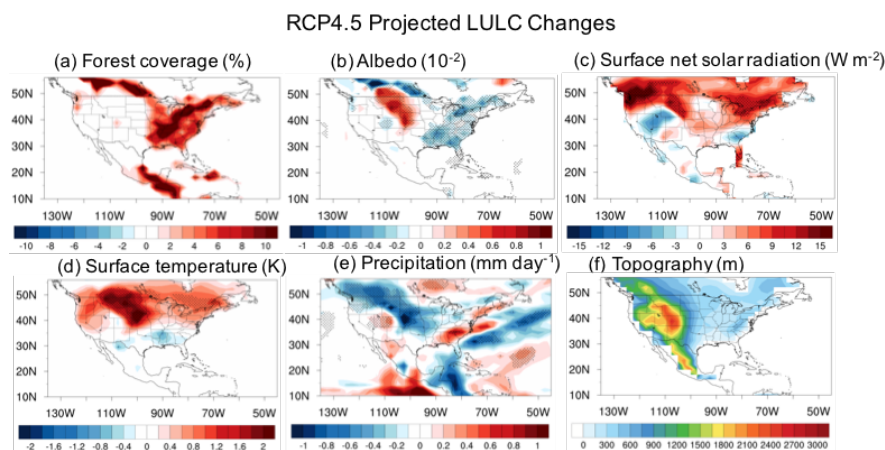
### 476 3.3.1 North America for RCP4.5 and RCP8.5

477 For RCP4.5, North America is subjected to intensive local-scale changes in  
478 LULC over the eastern US and southern Canada (Fig. 5a). Relatively large increases  
479 in surface ozone (Fig. 4a) and near-surface temperature (Fig. 4d) are found over a  
480 large continuous area in North America, including both the region with LULC  
481 changes and the region where LULC changes are minimal. We find that the intensive  
482 local-scale LULC changes could initiate local temperature change that can further  
483 impact larger-scale temperature over North America. For the intensive LULC changes  
484 region, the eastern US (Fig. 5a), reforestation results in substantial decreases in  
485 surface albedo (Fig. 5b), which leads to local increase in surface net solar radiation  
486 (Fig. 5c). Reforestation also leads to changes in latent and sensible heat fluxes, as well  
487 as surface longwave radiation (not shown here). The net effect is that local  
488 temperature increases accordingly. Significant increase of surface temperature is seen  
489 over the northeastern US (Fig. 5d). In the southeastern US, surface net solar radiation  
490 changes are much smaller, or even negative in some regions (Fig. 5c). Albedo effects  
491 of increasing surface net solar radiation appear to be mostly offset by the enhanced  
492 precipitation (Fig. 5e), cloud cover and latent heat, resulting in a modest net cooling at  
493 the surface (Fig. 5d).

494



495



496

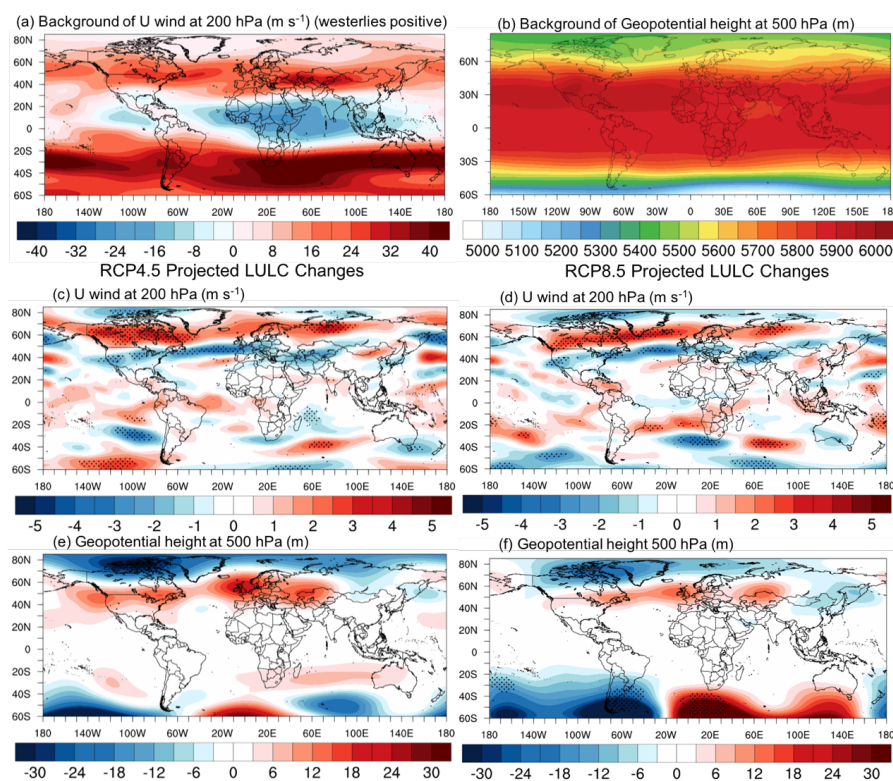
497 Figure 5. Changes in projected forest, simulated surface albedo, surface net solar radiation, surface  
498 temperature and precipitation during the boreal summer over the US due to RCP4.5 projected LULC  
499 change. Topography in this region is also shown.

500 It is noteworthy that temperature also increases significantly over the locations  
501 where the land use does not change, such as the Great Plains and Rocky Mountains in  
502 central-western US (Figs. 5a and 5d). The warming over these regions is likely related  
503 to atmospheric circulation changes over the northeastern US. Surface warming in  
504 relation to reduced albedo over the northeastern US can lead to enhanced upper-level  
505 westerlies immediately to the north, due to the thermal wind relation. Inspection of  
506 the anomalous zonal wind at 200 hPa indicates that the westerly jet core is displaced  
507 northward from its climatological position at  $\sim 50^{\circ}N$  (see Figs. 6a and 6c). Such a  
508 displacement of the jet can modulate the local stormtrack, which can further feedback  
509 onto the anomalous flow (Lau, 1988), favoring the formation of an anomalous high  
510 immediately to the south at 40-to- $50^{\circ}N$  over the continental US (Fig. 6e). Collocated  
511 with such a stationary high, there is enhanced (reduced) surface solar radiation  
512 (rainfall). The anomalous high in the RCP4.5 experiment can lead to sinking motion  
513 and hence low-level divergent wind that can substantially influence regional moisture



514 transport. The vertically integrated moisture fluxes at present-day conditions are  
515 shown in Fig. S1a, illustrating that moisture transport from the Gulf of Mexico and  
516 Pacific Ocean is deflected by the Rocky Mountains and toward the central-western  
517 US. In fact, the moisture flux pattern is significantly modified in the RCP4.5 runs,  
518 such that anomalous moisture flux divergence is found in the region (Fig. S1b),  
519 Overall the anomalous high (Fig. 6e), drier soil (Fig. 5b), reduced latent heat and  
520 precipitation (Fig. 5e), all act to promote warming over the central-western US region.

521 For the RCP8.5 run, surface ozone is also enhanced in North America (Fig.  
522 4e) and is again well correlated with near-surface warming (Fig. 4h). However, the  
523 ozone concentration increase is smaller than that in RCP4.5, presumably due to  
524 weaker LULC changes.



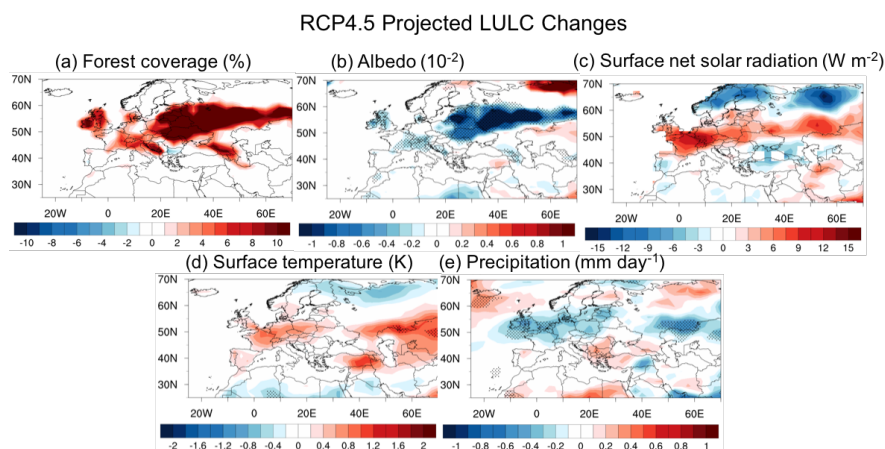
525



526 Figure 6. Present-day conditions and changes in zonal wind at 200 hPa and geopotential height at 500  
527 hPa during the boreal summer. Changes due to RCP4.5 projected LULC change are in middle-bottom  
528 left panel, while RCP8.5 in middle-bottom right panel.

### 529 3.3.2 Europe for RCP4.5 and RCP8.5

530 Over Europe substantial increases in surface ozone (Figs. 4a, e) and near-  
531 surface air temperature (Figs. 4d, h) are found due to RCP4.5 and RCP8.5 LULC  
532 changes. For RCP4.5, substantial reforestation occurs over Europe continental regions  
533 (Fig. 7a), which modifies regional surface energy balance and atmospheric  
534 circulation. Forest expansion reduces local albedo (Fig. 7b) and increases surface net  
535 solar radiation accordingly over Europe continental areas (Fig. 7c). Reforestation also  
536 leads to changes in latent heat and sensible heat fluxes (not shown here). Considering  
537 all surface energy components, the net surface energy budget yields a positive  
538 tendency and thus a surface temperature increase (Fig. 7d). The higher temperature is  
539 seen to be collocated with local surface ozone changes over the continent.



540  
541 Figure 7. Similar to Figure 4 but for Europe in RCP4.5.

542 Similar to the anomalous circulation over North America, in Europe there is  
543 also surface warming extending to the west of LULC changes for RCP 4.5. Again this  
544 is likely due to a similar mechanism in which the enhanced westerlies at about 55–



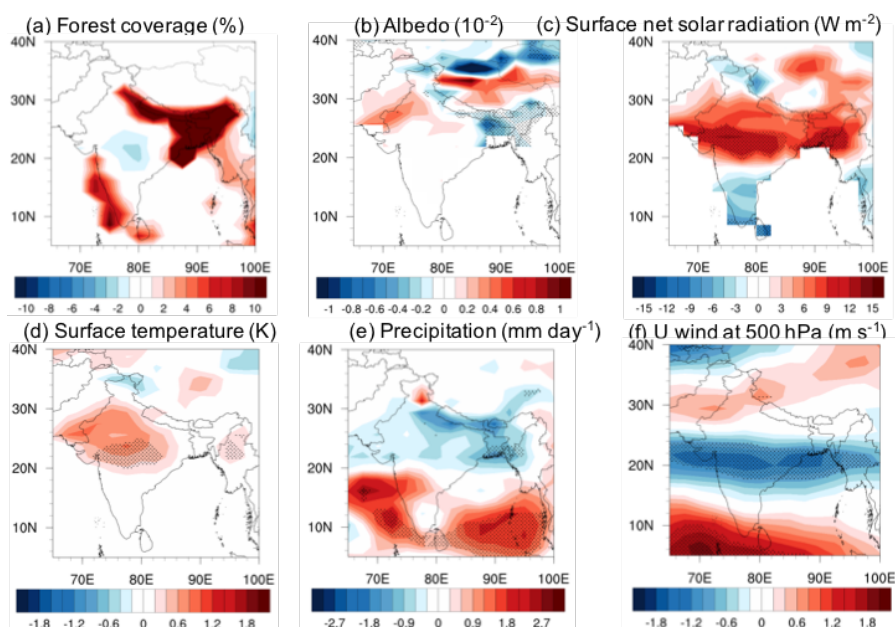
545 60°N (Fig. 6c); modified storm tracks and the anomalous high are acting in concert,  
546 leading to more subsidence in the European region that experiences increased surface  
547 net solar radiation (Fig. 7c), thus surface warming (Fig. 7d). For RCP8.5,  
548 reforestation occurs over limited areas of Europe (Figs. 2i, 1j, 1k); similar changes in  
549 the local climate and surface ozone are found, albeit with a relatively weak amplitude  
550 compared with their RCP8.5 counterparts.

### 551 3.3.3 India and China for RCP4.5 and RCP8.5

552 For RCP4.5, extensive reforestation occurs in northeastern and southwestern  
553 India (Fig. 8a). There is also a significant increase of surface ozone over northern  
554 India (Fig. 4a), collocated with warming (Fig. 4d). Again, temperature increase tends  
555 to occur west of the LULC changes (Fig. 8d), suggesting a mechanism of circulation  
556 changes similar to those operating in North America and Europe. The mid-  
557 tropospheric anomalous flow is characterized by an anticyclone between 20–30°N and  
558 suppressed rainfall therein (Figs. 8e, 8f), leading to more surface net radiation (Fig.  
559 8c). Thus in northern India there is significant surface warming (Fig. 8d) and  
560 enhanced surface ozone. Finally, in China extensive deforestation occurs for RCP4.5.  
561 Surface ozone shows a slightly decrease that could be caused by biogeochemical  
562 effects associated with LULC changes instead of biogeophysical effects. This region  
563 is characterized by a temperate climate, medium isoprene emission from temperate  
564 trees (Fig. 3a) and high anthropogenic NO<sub>x</sub> emissions (Fig. 3d). Changes from  
565 temperate trees to croplands further decrease isoprene emission and lead to significant  
566 ozone decreases, which largely offsets the effects of reduced dry deposition velocity  
567 (Fig. 4b). For RCP8.5, little change in surface ozone or temperature has been found in  
568 either country.



### RCP4.5 Projected LULC Changes



569

570 Figure 8. Similar to Figure 4 but for India in RCP4.5.

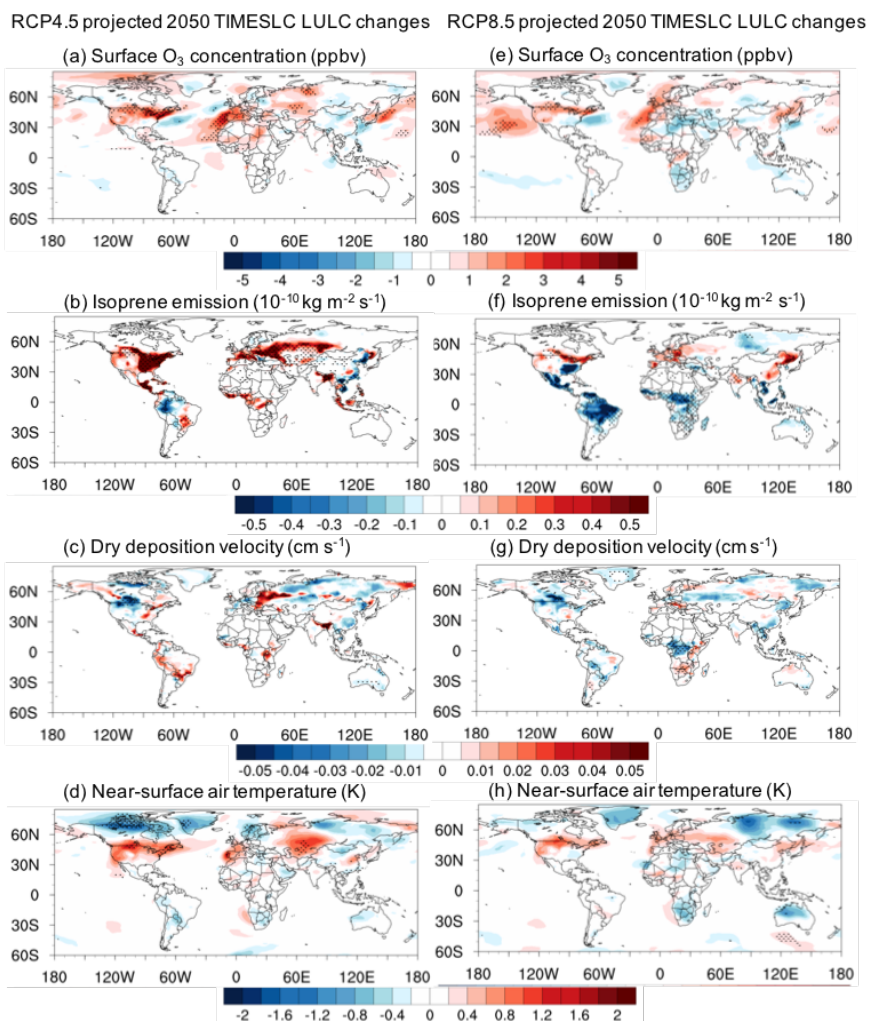
571 Overall, we find that biogeophysical effects can amplify surface ozone  
572 increases due to surface warming and circulation anomalies initiated by local LULC  
573 changes in several hotspots (Fig. 1). Our results of temperature changes are consistent  
574 with the previous study of Swann et al. (2012) that illustrated the local and remote  
575 climate effects of the northern mid-latitude reforestation. They conducted a model  
576 experiment with extreme afforestation, and found substantial warming in North  
577 America and Europe. In addition, Govindasamy and Caldeira (2001) also found  
578 surface cooling due to deforestation.



579 3.3.4 Time-sliced experiments versus transient experiments

580 In the Off-line configurations, we use time-sliced experiments for present-day  
581 LULC conditions in 2000 and future conditions in 2050. However, the LULC in On-  
582 line mode is transient with LULC changing annually and the atmosphere responds to  
583 such changes accordingly. For a paralleled comparison with Off-line mode, time-  
584 sliced runs in On-line mode are also conducted. Our results show that changes in  
585 ozone, near-surface air temperature, and other factors controlling ozone are similar  
586 between transient and time-sliced runs in the On-line mode (Fig. 9). The consistent  
587 model performance using transient and time-sliced LULC indicates that the LULC-  
588 forced signal is strong enough to cause changes in meteorology and ozone pollution,  
589 and the atmospheric responses and the biogeophysical effects are generally fast-  
590 responding at a quasi-steady state on timescales of years to decades with respect to  
591 the slow LULC changes.





592

593 Figure 9. Similar to Figure 3 but simulated from time-sliced configurations.

594

#### 595 4. Conclusions and Discussion

596 LULC continues to change along with future socioeconomic development and  
597 anthropogenic emission reduction strategies. These changes likely had, and will  
598 continue to have a large impact on air quality and climate. However, the impacts of  
599 LULC changes on surface ozone pollution are not fully understood, and the  
600 attribution to different LULC-mediated pathways is far from complete. Here, we



601 investigate and quantify specifically the biogeochemical effects (via modifying  
602 ozone-relevant chemical fluxes), biogeophysical effects (via modifying the overlying  
603 meteorological environment), and the integrated effects of LULC changes on surface  
604 ozone air quality.

605         We address the biogeochemical effects alone by performing CESM  
606 simulations with prescribed meteorology, and investigate the integrated effects using  
607 atmosphere-chemistry-land coupled configuration with dynamic meteorology. We  
608 find that the biogeochemical effects of changing isoprene emission and dry deposition  
609 following LULC changes mostly offset each other, resulting in only modest changes  
610 in ozone by up to 2 ppbv from 2000 to 2050. However, surface ozone can be  
611 significantly altered by up to 6 ppbv when considering the integrated effects  
612 associated with the LULC changes. In particular, the biogeophysical effects facilitated  
613 through temperature changes plays a critical role in shaping surface ozone. We find  
614 that temperature and surface ozone increases significantly in RCP4.5 over both  
615 regions with intensive LULC changes, such as the northeastern US, continental  
616 Europe and northeastern India, and regions with limited LULC changes, such as the  
617 central-western US, coastal Europe and northwestern India. The surface ozone  
618 changes due to future LULC change are comparable with anthropogenic emissions  
619 and climate, and thus should be taken into account in future research and policy  
620 planning.

621         The mechanisms behind the local temperature responses to LULC changes can  
622 be largely attributed to the radiative process of surface albedo changes and surface  
623 energy budget. Local temperature changes can further induce a regional circulation  
624 response, in particular the formation of anomalous stationary high-pressure systems  
625 and warming conditions over the mid-to-high northern latitudes in boreal summer.



626 Meanwhile, the anomalous high diverges moisture transport away from the region,  
627 inducing a series of feedbacks that result in generally drier and warmer conditions  
628 (Fig. 1).

629 Weaker responses of temperature as well as of surface ozone to LULC  
630 changes are found in RCP8.5 compared with those in RCP4.5. The different extent of  
631 temperature responses can be attributed to the location where LULC changes occur.  
632 For RCP4.5, LULC changes are most intense in the mid-latitude region of the  
633 Northern Hemisphere. In contrast, most LULC changes for RCP8.5 occur over the  
634 equatorial regions and Southern Hemisphere. Temperature responses to LULC  
635 changes may be less sensitive to tropical changes or changes over the Southern  
636 Hemisphere that is dominated by the vast oceanic expanse. Van der Molen et al  
637 (2011) using other models also found similar patterns, and named such climate  
638 responses to LULC changes as “tropical damping”. The classical theory of such  
639 “tropical damping” is associated with a decrease in cloud cover after deforestation,  
640 which then results in increased incoming radiation at the surface and a lower  
641 planetary albedo, both counteracting the increase in surface albedo with deforestation.

642 Our study has several limitations. First, the energy transport between the  
643 ocean and land has not been taken into account. Although using a fully interactive  
644 ocean component would increase the variability of simulated climate and decrease the  
645 signal-to-noise ratio in sensitivity experiments using small forcings, such as LULC  
646 changes (e.g., Davin and de Noblet-Ducoudre 2010, Brovkin et al., 2013), coupled  
647 atmosphere-ocean simulations are crucial for future climate change projections for the  
648 longer term (e.g., well past the end of the 21<sup>st</sup> century). In addition, future LULC  
649 projections in RCPs are predicted from the ensemble of socioeconomic and emission  
650 scenarios to match identified pathways of greenhouse gas concentrations. Large



651 uncertainties remain in such projections, calling for more skillful design of LULC-  
652 related metrics and the corresponding spatial patterns for better air quality predictions.  
653 Third, the biogeochemical effects of LULC on ozone in this study do not consider  
654 climatic changes that may arise when the carbon and nitrogen cycles are perturbed by  
655 LULC change, but only focus on the more immediate effects generated from LULC  
656 change such as isoprene emission and dry deposition, mostly due to model  
657 limitations. The full biogeochemical effects of LULC on ozone that include  
658 biogeochemical cycle-climate feedbacks will warrant further investigation but will  
659 foreseeably present greater challenges for process attribution and interpretation.

660       Furthermore, the overall effect of LULC changes is the residual outcome of  
661 the compensation between biogenic VOC emissions and dry deposition in off-line  
662 runs, which often change in the same direction following a given LULC change but  
663 have opposite effects on ozone. The overall sign of effect is thus particularly sensitive  
664 to model representation of these two processes. For instance, Val Martin et al. (2014)  
665 showed that replacing the default semi-empirical Wesely (1989) scheme of stomatal  
666 resistance with photosynthesis-based resistance calculated in CLM could enhance dry  
667 deposition velocity and reduce the original high biases in simulated summertime  
668 ozone in CESM. We have implemented this replacement in our simulations,  
669 essentially resulting in a higher sensitivity of surface ozone to LULC-induced dry  
670 deposition changes than other models with the semi-empirical scheme such as GEOS-  
671 Chem. The sensitivity of ozone to isoprene emission changes is also strongly  
672 dependent on the O<sub>3</sub>-NO<sub>x</sub>-VOC chemical mechanisms represented in models. For  
673 instance, CESM is found to be unable to properly simulate ozone in the southeastern  
674 US when NO<sub>x</sub> concentration decreases to lower levels during the 2000s (Brown-



675 Steiner et al., 2015), pointing to potential caveats in the simulated NO<sub>x</sub>-VOC emission  
676 ratios.

677 Our study highlights the complexity of LULC forcing and the importance of  
678 biogeophysical effects of LULC on surface ozone air quality, emphasizing the  
679 importance of LULC in atmospheric chemistry that could be as potentially important  
680 as anthropogenic emissions and climate. Our study can provide important reference  
681 for policy makers to consider the substantial roles of LULC in tackling air pollution  
682 and climate change, to develop a more comprehensive set of climatically relevant  
683 metrics for the management of the terrestrial biosphere, as well as to explore co-  
684 benefits among air pollution, climate change and LULC management strategies.

685

#### 686 **Author Contribution**

687 L. Wang designed the research, performed numerical simulations and the  
688 analysis, and wrote the draft; A. P. K. Tai, and C.-Y. Tam designed the research,  
689 performed the analysis, and wrote the draft; and all the authors contributed to the  
690 interpretation of the results and the writing of the paper.

691

#### 692 **Acknowledgments**

693 This work was supported by the Vice-Chancellor Discretionary Fund (Project  
694 ID: 4930744) from The Chinese University of Hong Kong (CUHK) given to the  
695 Institute of Environment, Energy and Sustainability.

696

697



698 **References**

- 699 Avnery S., Mauzerall D. L., Liu J., and Horowitz L. W.: Global crop yield reductions  
700 due to surface ozone exposure: 2. Year 2030 potential crop production losses and  
701 economic damage under two scenarios of O<sub>3</sub> pollution, *Atmos. Environ.*, 45, 2297-  
702 2309, <https://doi.org/10.1016/j.atmosenv.2011.01.002>, 2011.
- 703 Betts, R. A.: Biogeophysical impacts of land use on present-day climate: near-surface  
704 temperature change and radiative forcing, *Atmos. Sci. Lett.*, 2, 39-51,  
705 <https://doi.org/10.1006/asle.2001.0023>, 2001.
- 706 Bonan, G.: Forests, Climate, and Public Policy: A 500-Year Interdisciplinary  
707 Odyssey, *Annu. Rev. Ecol. Evol. Syst.*, 47, 97-121, <https://doi.org/10.1146/annurev-ecolsys-121415-032359>, 2016.
- 709 Brovkin, V., Boysen L., Arora, V. K., Boisier, J. P., Cadule, P., Chini, L., Claussen,  
710 M., Friedlingstein, P., Gayler, V., van den Hurk, B. J. J. M., Hurtt, G. C., Jones, C. D.,  
711 Kato, E., de Noblet-Ducoudré, N., Pacifico, F., Pongratz, J., and Weiss, M.: Effect of  
712 anthropogenic land-use and land-cover changes on climate and land carbon storage in  
713 CMIP5 projections for the twenty-first century, *J. Clim.*, 26, 6859-6881,  
714 <https://doi.org/10.1175/JCLI-D-12-00623.1>, 2013.
- 715 Brown-Steiner, B., Hess, P. G., and Lin, M. Y.: On the capabilities and limitations of  
716 GCM simulations of summertime regional air quality: A diagnostic analysis of  
717 ozone and temperature simulations in the US using CESM CAM-Chem, *Atmospheric  
718 Environment*, 101, 134-148, <https://doi.org/10.1016/j.atmosenv.2014.11.001>, 2015.
- 719 Chase, T., Pielke, R., Kittel, T., Nemani, R., and Running, S.: Sensitivity of a general  
720 circulation model to global changes in leaf area index, *J. Geophys. Res.*, 101 (D3),  
721 7393-7408, <https://doi.org/10.1029/95JD02417>, 1996.



722 Doherty, R. M., Wild, O., Shindell, D. T., Zeng, G., MacKenzie, I. A., Collins, W. J.,  
723 Fiore, A. M., Stevenson, D. S., Dentener, F. J., Schultz M. G., Hess, P., Derwent, R.  
724 G., and Keating, T. J.: Impacts of climate change on surface ozone and  
725 intercontinental ozone pollution: A multi-model study, *J. Geophys. Res. Atmos.*, 118,  
726 1-20, <https://doi.org/10.1002/jgrd.50266>, 2013.

727 Emmons, L. K., Walters, S., Hess, P. G., Lamarque, J.-F., Pfister, G. G., Fillmore, D.,  
728 Granier, C., Guenther, A., Kinnison, D., Laepple, T., Orlando, J., Tie, X., Tyndall, G.,  
729 Wiedinmyer, C., Baughcum, S. L., and Kloster, S.: Description and evaluation of the  
730 Model for Ozone and Related chemical Tracers, version 4 (MOZART-4), *Geosci.*  
731 *Model Dev.*, 3, 43-67, <https://doi.org/10.5194/gmd-3-43-2010>, 2010.

732 Fiore, A. M., Horowitz, L. W., Purves, D. W., Levy II, H., Evans, M. J., Wang, Y.,  
733 Li, Q., and Yantosca, M.: Evaluating the contribution of changes in isoprene  
734 emissions to surface ozone trends over the eastern United States, *J. Geophys. Res.*  
735 *Atmos.*, 110, D12303, <https://doi.org/10.1029/2004JD005485>, 2005.

736 Fiore, A. M., Naik, V., Spracklen, D. V., Steiner, A., Unger, N., Prather, M., and  
737 Bergmann, D.: Global air quality and climate, *Chem. Soc. Rev.*, 41, 6663-6683, DOI:  
738 10.1039/C2CS35095E, 2012.

739 Fu, Y., and Tai, A. P. K.: Impact of climate and land cover changes on tropospheric  
740 ozone air quality and public health in East Asia between 1980 and 2010, *Atmos.*  
741 *Chem. Phys.*, 15, 10093-10106, <https://doi.org/10.5194/acp-15-10093-2015>, 2015.

742 Ganzeveld, L., Bouwman, L., Stehfest, E., van Vuuren, D. P., Eickhout, B., and  
743 Lelieveld, J.: Impact of future land use and land cover changes on atmospheric  
744 chemistry-climate interactions, *J. Geophys. Res. Atmos.*, 115, D23301,  
745 <https://doi.org/10.1029/2010JD014041>, 2010.



746 Govindasamy, B., and Caldeira, K.: Land use changes and Northern Hemisphere  
747 cooling, *Geophys. Res. Lett.*, 28, 291-294, <https://doi.org/10.1029/2000GL006121>,  
748 2001.

749 Guenther, A. B., Jiang, X., Heald, C. L., Sakulyanontvittaya, T., Duhl, T., Emmons,  
750 L. K., and Wang, X.: The Model of Emissions of Gases and Aerosols from Nature  
751 version 2.1 (MEGAN2.1): an extended and updated framework for modeling biogenic  
752 emissions, *Geosci. Model Dev.*, 5, 1471-1492, [https://doi.org/10.5194/gmd-5-1471-](https://doi.org/10.5194/gmd-5-1471-2012)  
753 2012, 2012.

754 Henderson-Sellers, A., Dickinson, R. E., Durbidge, T. B., Kennedy, P. J., McGuffie,  
755 K., and Pitman, A. J.: Tropical deforestation: Modeling local- to regional-scale  
756 climate change, *J. Geophys. Res. Atmos.*, 98, 7289-7315,  
757 <https://doi.org/10.1029/92JD02830>, 1993.

758 Heald C. L., Henze, D. K., Horowitz, L. W., Feddema, J., Lamarque, J.-F., Guenther,  
759 A., Hess, P. G., Vitt, F., Seinfeld, J. F., Goldstein, A. H., and Fung, I.: Predicted  
760 change in global secondary organic aerosol concentrations in response to future  
761 climate, emissions, and land use change, *J. Geophys. Res.*, 113, D05211,  
762 [doi:10.1029/2007JD009092](https://doi.org/10.1029/2007JD009092), 2008.

763 Heald, C. L., and Spracklen, D. V.: Land use change impacts on air quality and  
764 climate, *Chem. Rev.*, 115, 4476-4496, <https://doi.org/10.1021/cr500446g>, 2015.

765 Heald, C. L., and Geddes, J. A.: The impact of historical land use change from 1850  
766 to 2000 on secondary particulate matter and ozone, *Atmos. Chem. Phys.*, 16, 14997-  
767 15010, <https://doi.org/10.5194/acp-16-14997-2016>, 2016.

768 Hurtt, G. C., Chini, L. P., Frohling, S., Betts, R. A., Feddema, J., Fischer, G., Fisk, J.  
769 P., Hibbard, K., Houghton, R. A., Janetos, A., Jones, C. D., Kindermann, G.,  
770 Kinoshita, T., Goldewijk, K. K., Riahi, K., Shevliakova, E., Smith, S., Stehfest, E.,





771 Thomson, A., Thornton, P., van Vuuren, D. P., and Wang, Y. P.: Harmonization of  
772 land-use scenarios for the period 1500–2100: 600 years of global gridded annual land-  
773 use transitions, wood harvest, and resulting secondary lands, *Climatic Change*, 109,  
774 117-161, DOI:10.1007/s10584-011-0153-2, 2011.

775 Jacob, D. J., and Winner, D. A.: Effect of climate change on air quality, *Atmos.*  
776 *Environ.*, 43, 51-63, <https://doi.org/10.1016/j.atmosenv.2008.09.051>, 2009.

777 Jerrett, M., Burnett, R. T., Pope, C. A., Ito, K., Thurston, G., Krewski, D., Shi, Y.,  
778 Calle, E., and Thun, M.: Long-Term Ozone Exposure and Mortality, *New Engl. J.*  
779 *Med.*, 360, 1085-1095, DOI: 10.1056/NEJMoa0803894, 2009.

780 Jiang, X., Wiedinmyer, C., Chen, F., Yang, Z.-L., and Lo, J. C.-F.: Predicted impacts  
781 of climate and land use change on surface ozone in the Houston, Texas, area, *J.*  
782 *Geophys. Res.*, 113, D20312, <https://doi.org/10.1029/2008JD009820>, 2008.

783 Kang, D., Aneja, V. P., Mathur, R., and Ray, J. D.: Nonmethane hydrocarbons and  
784 ozone in three rural southeast United States national parks: A model sensitivity  
785 analysis and comparison to measurements, *J. Geophys. Res.*, 108, 4604,  
786 <https://doi.org/10.1029/2002JD003054>, 2003.

787 Lamarque, J.-F., Bond, T. C., Eyring, V., Granier, C., Heil, A., Klimont, Z., Lee, D.,  
788 Liousse, C., Mieville, A., Owen, B., Schultz, M. G., Shindell, D., Smith, S. J.,  
789 Stehfest, E., Van Aardenne, J., Cooper, O. R., Kainuma, M., Mahowald, N.,  
790 McConnell, J. R., Naik, V., Riahi, K., and van Vuuren, D. P.: Historical (1850-2000)  
791 gridded anthropogenic and biomass burning emissions of reactive gases and aerosols:  
792 methodology and application, *Atmos. Chem. Phys.*, 10, 7017-7039,  
793 <https://doi.org/10.5194/acp-10-7017-2010>, 2010.

794 Lamarque, J. F., Emmons, L. K., Hess, P. G., Kinnison, D. E., Tilmes, S., Vitt, F.,  
795 Heald, C. L., Holland, E. A., Lauritzen, P. H., Neu, J., Orlando, J. J., Rasch, P. J., and



796 Tyndall, G. K.: CAM-chem: description and evaluation of interactive atmospheric  
797 chemistry in the Community Earth System Model, *Geosci. Model Dev.*, 5, 369-411,  
798 <https://doi.org/10.5194/gmd-5-369-2012>, 2012.

799 Lapina, K., Henze, D. K., Milford, J. B., Huang, M., Lin, M., Fiore, A. M.,  
800 Carmichael, G., Pfister, G. G., and Bowman, K.: Assessment of source contributions  
801 to seasonal vegetative expo- sure to ozone in the US, *J. Geophys. Res. Atmos.*, 119,  
802 324-340, <https://doi.org/10.1002/2013JD020905>, 2014.

803 Lathièrè, J., Hauglustaine, D. A., Friend A. D., de Noblet-Ducoudré, N., Viovy N.,  
804 and Folberth, G. A.: Impact of climate variability and land use changes on global  
805 biogenic volatile organic compound emissions, *Atmos. Chem. Phys.*, 6, 2129-2146,  
806 <https://doi.org/10.5194/acp-6-2129-2006>, 2006.

807 Lawrence, D. M., Oleson, K. W., Flanner, M. G., Thornton, P. E., Swenson, S. C.,  
808 Lawrence, P. J., Zeng, X., Yang, Z.-L., Levis, S., Sakaguchi, K., Bonan, G. B., and  
809 Slater, A. G.: Parameterization Improvements and Functional and Structural  
810 Advances in Version 4 of the Community Land Model, *J. Adv. Model. Earth Syst.*, 3,  
811 M03001, <https://doi.org/10.1029/2011MS00045>, 2011.

812 Lawrence, P. J., Feddema, J. J., Bonan, G. B., Meehl, G. A., O'Neill, B. C., Levis, S.,  
813 Lawrence, D. M., Oleson, K. W., Kluzek, E., Lindsay, K., and Thorton, P. E.:  
814 Simulating the Biogeochemical and Biogeophysical Impacts of Transient Land Cover  
815 Change and Wood Harvest in the Community Climate System Model (CCSM4) from  
816 1850 to 2100, *J. Climate.*, 25, 3071-3095, <https://doi.org/10.1175/JCLI-D-11-00256.1>,  
817 2012.

818 Lau, N.-C.: Variability of the observed midlatitude storm tracks in relation to low-  
819 frequency change in the circulation pattern, *J. Atmos. Sci.*, 45, 2718-2743,  
820 [https://doi.org/10.1175/1520-0469\(1988\)045<2718:VOTOMS>2.0.CO;2](https://doi.org/10.1175/1520-0469(1988)045<2718:VOTOMS>2.0.CO;2), 1988.



821 Lin, M., Horowitz, L. W., Payton, R., Fiore, A. M., and Tonnesen G.: US surface  
822 ozone trends and extremes from 1980 to 2014: quantifying the roles of rising Asian  
823 emissions, domestic controls, wildfires, and climate, *Atmos. Chem. Phys.*, 17, 2943-  
824 2970, <https://doi.org/10.5194/acp-17-2943-2017>, 2017.

825 Malley, C. S., Henze, D. K., Kuylenstierna, J. C. I., Vallack, H. W., Davila, Y.,  
826 Anenberg, S. C., Turner, M. C., and Ashmore, M. R.: Updated global estimates of  
827 respiratory mortality in adults  $\geq 30$  years of age attributable to long-term ozone  
828 exposure, *Environ. Health Perspect.*, 125, 087021, doi: 10.1289/EHP1390, 2017.

829 Myhre, G., et al.: Anthropogenic and Natural Radiative Forcing. In: *Climate Change*  
830 *2013: The Physical Science Basis. Contribution of Working Group I to the Fifth*  
831 *Assessment Report of the Intergovernmental Panel on Climate Change* (Stocker, T.F.,  
832 et al., (eds.)). Cambridge University Press, Cambridge, United Kingdom and New  
833 York, NY, USA, 2013.

834 Oleson, K. W., Lawrence D. W., and Bonan, G. B.: Technical description of version  
835 4.5 of the Community Land Model (CLM). NCAR Technical Note NCAR/TN-  
836 503+STR, National Centre for Atmospheric Research, Boulder, USA, 2013.

837 Parrish, D. D., Lamarque, J. F., Naik, V., Horowitz, L., Shindell, D. T., Staehelin, J.,  
838 Derwent, R., Cooper, O. R., Tanimoto, H., Volz-Thomas, A., and Gilje, S.: Long-  
839 term changes in lower tropospheric baseline ozone concentrations: Comparing  
840 chemistry-climate models and observations at northern midlatitudes, *J. Geophys. Res.*  
841 *Atmos.*, 119, 5719-5736, <https://doi.org/10.1002/2013JD021435>, 2014.

842 Pfister, G. G., Emmons, L. K., Hess, P. G., Lamarque, J.-F., Orlando, J. J., Walters,  
843 S., Guenther, A., Palmer, P. I., and Lawrence, P. J.: Contribution of isoprene to  
844 chemical budgets: A model tracer study with the NCAR CTM MOZART-4, *J.*  
845 *Geophys. Res.*, 113, D05308, <https://doi.org/10.1029/2007JD008948>, 2008.



846 Pitman, A. J., de Noblet-Ducoudre, N., Cruz, F. T., Davin, E. L., Bonan, G. B.,  
847 Brovkin, V., Claussen, M., Delire, C., Ganzeveld, L., Gayler, V., van den Hurk, B.,  
848 Lawrence, P. J., van der Molen, M. K., Muller, C., Reick, C. H., Seneviratne, S. I.,  
849 Strengers, B. J., and Voldoire, A.: Uncertainties in climate responses to past land  
850 cover change: First results from the LUCID intercomparison study, *Geophys. Res.*  
851 *Lett.*, 36, L14814, <https://doi.org/10.1029/2009GL039076>, 2009.  
852 Porter, W. C., Heald, C. L., Cooley, D., and Russell, B.: Investigating the observed  
853 sensitivities of air-quality extremes to meteorological drivers via quantile regression,  
854 *Atmos. Chem. Phys.*, 15, 10349-10366, <https://doi.org/10.5194/acp-15-10349-2015>,  
855 2015.  
856 Pusede, S. E., Steiner, A. L., and Cohen, R. C.: Temperature and recent trends in the  
857 chemistry of continental surface ozone, *Chem. Rev.*, 115, 3898-3918,  
858 <https://doi.org/10.1021/cr5006815>, 2015.  
859 Rayner, N. A., Parker, D. E., Horton, E. B., Folland, C. K., Alexander, L. V., Rowell,  
860 D. P., Kent, E. C., and Kaplan, A.: Global analyses of sea surface temperature, sea  
861 ice, and night marine air temperature since the late nineteenth century, *J. Geophys.*  
862 *Res. Atmos.*, 108, D002670, <https://doi.org/10.1029/2002JD002670>, 2003.  
863 Riahi, K., Grübler, A., and Nakicenovic, N.: Scenarios of long-term socio-economic  
864 and environmental development under climate stabilization, *Technol. Forecast. Soc.*  
865 *Change*, 74, 887-935, <https://doi.org/10.1016/j.techfore.2006.05.026>, 2007.  
866 Riahi, K., Krey, V., Rao, S., Chirkov, V., Fischer, G., Kolp, P., Kindermann, G.,  
867 Nakicenovic, N., and Rafai, P.: RCP8.5-exploring the consequence of high emission  
868 trajectories, *Climatic Change*, 109:33, <https://doi.org/10.1007/s10584-011-0149-y>,  
869 2011.



870 Ramankutty, N., Evan, A. T., Monfreda, C., and Foley, J. A.: Farming the planet: 1.  
871 Geographic distribution of global agricultural lands in the year 2000, *Glob.*  
872 *Biogeochem. Cyc.*, 22, GB1003, <https://doi.org/10.1029/2007GB002952>, 2008.  
873 Sadiq, M., Tai, A. P. K., Lombardozzi, D., and Val Martin, M.: Effects of ozone-  
874 vegetation coupling on surface ozone air quality via biogeochemical and  
875 meteorological feedbacks, *Atmos. Chem. Phys.* 17, 3055-3066,  
876 <https://doi.org/10.5194/acp-17-3055-2017>, 2017.  
877 Schnell, J. L., Prather, M. J., Josse, B., Naik, V., Horowitz, L. W., Zeng, G., Shindell,  
878 D. T., and Faluvegi, G.: Effect of climate change on surface ozone over North  
879 America, Europe, and East Asia, *Geophys. Res. Lett.*, 43, 3509-3518,  
880 <https://doi.org/10.1002/2016GL068060>, 2016.  
881 Squire, O. J., Archibald, A. T., Abraham, N. L., Beerling, D. J., Hewitt, C. N.,  
882 Lathièrè, J., Pike, R. C., Telford, P. J., and Pyle, J. A.: Influence of future climate and  
883 cropland expansion on isoprene emissions and tropospheric ozone, *Atmos. Chem.*  
884 *Phys.*, 14, 1011-1024, <https://doi.org/10.5194/acp-14-1011-2014>, 2014.  
885 Shen, L., Mickley, L. J., and Gilleland, E.: Impact of increasing heat waves on US  
886 ozone episodes in the 2050s: Results from a multimodel analysis using extreme value  
887 theory, *Geophys. Res. Lett.*, 43, 4017-4025, <https://doi.org/10.1002/2016GL068432>,  
888 2016.  
889 Swann, A. L. S., Fung, I. Y., and Chiang, J. C. H.: Mid-latitude afforestation shifts  
890 general circulation and tropical precipitation, *Proc. Natl. Acad. Sci., USA*, 109, 712-  
891 716, <https://doi.org/10.1073/pnas.1116706108>, 2012.  
892 Tai, A. P. K., Mickley, L. J., Heald, C. L., and Wu, S.: Effect of CO<sub>2</sub> inhibition on  
893 biogenic isoprene emission: Implications for air quality under 2000 to 2050 changes



894 in climate, vegetation, and land use, *Geophys. Res. Lett.*, 40, 3479-3483,  
895 <https://doi.org/10.1002/grl.50650>, 2013.

896 Tai, A. P. K., Val Martin, M. and Heald, C. L.: Threat to Future Global Food Security  
897 from Climate Change and Ozone Air Pollution, *Nat. Clim. Change*, 4, 817-821,  
898 <https://doi.org/10.1038/nclimate2317>, 2014.

899 Tai, A. P. K., and Val Martin, M.: Impacts of ozone air pollution and temperature  
900 extremes on crop yields: Spatial variability, adaptation and implications for future  
901 food security, *Atmos. Environ.*, 169, 11-21, DOI10.1016/j.atmosenv.2017.09.002,  
902 2017.

903 Taylor, K. E., Stouffer, R. J., and Meehl, G. A.: An overview of CMIP5 and the  
904 experiment design, *Bull. Am. Meteorol. Soc.*, 93, 485-498,  
905 <https://doi.org/10.1175/BAMS-D-11-00094.1>, 2012.

906 Thomson, A. M., Calvin, K. V., Smith, S. J., Kyle, G. P., Volke, A., Patel, P.,  
907 Delgado-Arias, S., and Bond-Lamberty, B.: RCP4.5: a pathway for stabilization of  
908 radiative forcing by 2100, *Climatic Change*, 109, 77-94,  
909 <https://doi.org/10.1007/s10584-011-0151-4>, 2011.

910 Tian, H., Ren, W., Tao, B., Sun, G., Chappelka, A., Wang, X., Pan, S., Yang, J., Liu,  
911 J., Felzer, B., Melillo, J., and Reilly, J.: Climate extremes and ozone pollution: a  
912 growing threat to China's food security, *Ecosystem Health and Sustainability*, 2,  
913 e01203, <https://doi.org/10.1002/ehs2.1203>, 2016.

914 Tilmes, S.: GEOS5 Global Atmosphere Forcing Data. Research Data Archive at the  
915 National Center for Atmospheric Research, Computational and Information Systems  
916 Laboratory, <http://rda.ucar.edu/datasets/ds313.0/>, 2016.

917 Val Martin, M., Heald, C. L., and Arnold, S. R.: Coupling dry deposition to  
918 vegetation phenology in the Community Earth System Model: Implications for the



919 simulation of surface O<sub>3</sub>, *Geophys. Res. Lett.*, 41, 2988-2996,  
920 <https://doi.org/10.1002/2014GL059651>, 2014.

921 Val Martin, M., Heald, C. L., Lamarque, J.-F., Tilmes, S., Emmons, L. K., and  
922 Schichtel, B. A.: How emissions, climate, and land use change will impact mid-century  
923 air quality over the United States: a focus on effects at national parks, *Atmos. Chem.*  
924 *Phys.*, 15, 2805-2823, <https://doi.org/10.5194/acp-15-2805-2015>, 2015.

925 van der Molen, M. K., van den Hurk, B. J. J. M., and Hazeleger, W.: A dampened  
926 land use change climate response towards the tropics, *Clim. Dyn.*, 37, 2035-2043,  
927 <https://doi.org/10.1007/s00382-011-1018-0>, 2011.

928 Van Vuuren, D. P., den Elzen, M. G. J., Lucas, P. L., Eickhout, B., Strengers, B. J.,  
929 van Ruijven, B., Wonink, S., and van Houdt, R.: Stabilizing greenhouse gas  
930 concentrations at low levels: an assessment of reduction strategies and costs, *Climatic*  
931 *Change*, 81, 119-159, <https://doi.org/10.1007/s10584-006-9172-9>, 2007.

932 van Vuuren, D. P., Edmonds, J., Kainuma, M., Riahi, K., Thomson, A., Hibbard, K.,  
933 Hurtt, G. C., Kram, T., Krey, V., Lamarque, J. F., Masui, T., Meinshausen, M.,  
934 Nakicenovic, N., Smith, S. J., and Rose, S. K.: The representative concentration  
935 pathways: an overview, *Climatic Change*, 109, 5-31, [https://doi.org/10.1007/s10584-](https://doi.org/10.1007/s10584-011-0148-z)  
936 [011-0148-z](https://doi.org/10.1007/s10584-011-0148-z), 2011.

937 Verbeke, T., Lathière, J., Szopa, S., and de Noblet-Ducoudré, N.: Impact of future  
938 land-cover changes on HNO<sub>3</sub> and O<sub>3</sub> surface dry deposition, *Atmos. Chem. Phys.*, 15,  
939 13555-13568, <https://doi.org/10.5194/acp-15-13555-2015>, 2015.

940 von Kuhlmann, R., Lawrence, M. G., Poschl, U., and Crutzen, P. J.: Sensitivities in  
941 global scale modeling of isoprene, *Atmos. Chem. Phys.*, 4, 1-17,  
942 <https://doi.org/10.5194/acp-4-1-2004>, 2004.



943 Wang, Y., Zhang, Y., Hao, J., and Luo, M.: Seasonal and spatial variability of surface  
944 ozone over China: contributions from background and domestic pollution, *Atmos.*  
945 *Chem. Phys.*, 11, 3511-3525, <https://doi.org/10.5194/acp-11-3511-2011>, 2011.

946 Wang, Y., Shen, L., Wu, S., Mickley, L., He, J., and Hao, J.: Sensitivity of surface  
947 ozone over China to 2000-2050 global changes of climate and emissions, *Atmos.*  
948 *Environ.*, 75, 374-382, <https://doi.org/10.1016/j.atmosenv.2013.04.045>, 2013.

949 Wesely, M.: Parameterization of surface resistances to gaseous dry deposition in  
950 regional-scale numerical models, *Atmos. Environ.*, 23, 1293-1304,  
951 [https://doi.org/10.1016/0004-6981\(89\)90153-4](https://doi.org/10.1016/0004-6981(89)90153-4), 1989.

952 Wise, M., Calvin, K., Thomson, A., Clarke, L., Bond-Lamberty, B., Sands, R., Smith,  
953 S., J., Janetos, A., and Edmonds, J.: Implication of limiting CO<sub>2</sub> concentrations for  
954 land use and energy, *Science*, 324, 1183-1186, DOI: 10.1126/science.1168475,  
955 2009a.

956 Wise, M., Calvin, K., Thomson, A., Clarke, L., Sands, R., Smith, S. J., Janetos, A.,  
957 and Edmonds, J.: The Implications of Limiting CO<sub>2</sub> Concentrations for Agriculture,  
958 Land-use Change Emissions, and Bioenergy, Technical Report, DOE Pacific  
959 Northwest National Laboratory, 2009b.

960 Wong, A. Y. H., Tai, A. P. K., and Ip, Y.-Y.: Attribution and statistical  
961 parameterization of the sensitivity of surface ozone to changes in leaf area index  
962 based on a chemical transport model, *J. Geophys. Res. Atmos.*, 123, 1883-1898,  
963 <https://doi.org/10.1002/2017JD027311>, 2018.

964 World Health Organization: WHO Air quality guidelines for particulate matter,  
965 ozone, nitrogen dioxide and sulfur dioxide, Global update 2005, Summary of risk  
966 assessment, 2005.





967 ([http://apps.who.int/iris/bitstream/10665/69477/1/WHO\\_SDE\\_PHE\\_OEH\\_06.02\\_eng](http://apps.who.int/iris/bitstream/10665/69477/1/WHO_SDE_PHE_OEH_06.02_eng)  
968 .pdf).

969 Wu, S., Mickley, L. J., Kaplan, J. O., and Jacob, D. J.: Impacts of changes in land use  
970 and land cover on atmospheric chemistry and air quality over the 21st century, *Atmos.*  
971 *Chem. Phys.*, 12, 1597-1609, <https://doi.org/10.5194/acp-12-1597-2012>, 2012.

972 Xue, L., Wang, T., Louie, P. K. K., Luk, C. W. Y., Blake, D. R., and Xu, Z.:  
973 Increasing external effects negate local efforts to control ozone air pollution: A case  
974 study of Hong Kong and implications for other Chinese cities, *Environ. Sci. Technol.*,  
975 48, 10769-10775, <https://doi.org/10.1021/es503278g>, 2014.

976 Yienger, J. J., and Levy II H.: Empirical model of global soil-biogenic  $\text{NO}_x$   
977 emissions, *J. Geophys. Res. Atmos.*, 100, 11447-11464,  
978 <https://doi.org/10.1029/95JD00370>, 1995.

979 Yue, X. and Unger, N.: Ozone vegetation damage effects on gross primary  
980 productivity in the United States, *Atmos. Chem. Phys.*, 14, 9137-9153,  
981 <https://doi.org/10.5194/acp-14-9137-2014>, 2014.

982 Zhang, Q., Yuan, B., Shao, M., Wang, X., Lu, S., Lu, K., Wang, M., Chen, L., Chang,  
983 C.-C., and Liu, S. C.: Variations of ground-level  $\text{O}_3$  and its precursors in Beijing in  
984 summertime between 2005 and 2011, *Atmos. Chem. Phys.*, 14, 6089-6101,  
985 <https://doi.org/10.5194/acp-14-6089-2014>, 2014.

986 Zhou, D., Ding, A., Mao, H., Fu, C., Wang, T., Chan, L. Y., Ding, K., Zhang, Y., Liu,  
987 J., Lu, A., Hao, N.: Impacts of the East Asian monsoon on lower tropospheric ozone  
988 over coastal South China, *Environ. Res. Lett.*, 8, 044011, doi:10.1088/1748-  
989 9326/8/4/044011, 2013.

990